Journal of
Manufacturing and Materials Processing

MDPI

Article

Pressure-Based Feedback Control for Reducing Extrusion Pulsation in a Single-Screw Direct-Extrusion 3D Printer

Jan-Uwe R. Schmidt [1,*,†], Jens Jähnicke [2,3,†], Sebastian Brühl [1], Ralf Keimer [1], Maik Titze [1], Hans Peter Monner [1] and Henning Zeidler [2]

[1] German Aerospace Center (DLR), Institute of Lightweight Systems, 38108 Braunschweig, Germany; ralf.keimer@dlr.de (R.K.); maik.titze@dlr.de (M.T.); hans.monner@dlr.de (H.P.M.)
[2] TU Bergakademie Freiberg, Faculty of Mechanical, Process and Energy Engineering, Institute of Machine Elements, Design and Manufacturing, Agricolastraße 1, 09599 Freiberg, Germany; jens.jaehnicke@siemens.com (J.J.); henning.zeidler@imkf.tu-freiberg.de (H.Z.)
[3] Siemens AG, Digital Industries, Automation, Sales, Domaine Management, Horizontal Additive Manufacturing, Clemens-Winkler-Straße 3, 09116 Chemnitz, Germany
* Correspondence: jan-uwe.schmidt@dlr.de; Tel.: +49-531-295-1512
† These authors contributed equally to this work.

Abstract

Weight- and cost-optimized extruders are used in additive manufacturing. Material-flow pulsation is a major challenge in screw-based material extrusion additive manufacturing, as it reduces dimensional accuracy and print quality. This study investigates the relationship between internal nozzle pressure and material flow in a polymer-feeding single-screw extruder and evaluates pressure-based closed-loop control as a means of reducing extrusion pulsation. An experimental setup comprising an integrated nozzle-pressure sensor, a synchronized conveyor belt, and a laser-line scanner was developed to simultaneously measure nozzle pressure and the cross-sectional area of the extruded strand. Based on volumetric setpoints derived from the G-code, corrected extruder motor commands were generated and implemented using proportional (P) and proportional–integral (PI) pressure control. The experimental results reveal a strong correlation between internal nozzle pressure and the resulting strand cross-section. The strand modulation correlated with screw rotation could be almost completely eliminated. At the investigated medium extrusion speed, pressure feedback reduced the remaining strand cross-sectional modulation to approximately 33% of the uncontrolled reference condition. Using PLA (Polylactic Acid) material the presented approach demonstrates that pressure-based feedback control is a practical method for improving process stability and extrusion quality in screw-based additive manufacturing and provides a foundation for future advanced control strategies.

Keywords: material extrusion additive manufacturing; single-screw extruder; pressure control; closed-loop control; process monitoring; flow pulsation; polymer extrusion; in situ sensing

Check for updates

Academic Editors: Narges Dialami and Shuo Yin

Received: 22 July 2026
Revised: 23 October 2026
Accepted: 26 October 2026
Published: 1 November 2026

Copyright: © 2026 by the authors. Licensee MDPI, Basel, Switzerland. This article is an open access article distributed under the terms and conditions of the Creative Commons Attribution (CC BY) license.

1. Introduction

Additive manufacturing (AM) is increasingly used in industrial applications, with large-scale material extrusion commonly implemented using robotic systems equipped with polymer extrusion heads [1,2]. Depending on the application, these systems employ different extrusion concepts, including single- and twin-screw extruders and melt-pump-based systems. Screw-based extrusion enables the processing of polymer granules at comparatively high material throughput. However, variations in melt pressure and material

flow can occur during continuous extrusion, resulting in fluctuations in the deposited material and variations in strand geometry [1–5].

A stable volumetric flow is an important prerequisite for achieving a consistent deposited strand geometry and uniform wall dimensions. Variations in material flow can therefore result in variations in strand width and cross-sectional area and may contribute to dimensional deviations and non-uniform material deposition. For adjacent deposited strands, insufficient or excessive material deposition may additionally result in local gaps or material accumulation. Consequently, reducing extrusion pulsation is important for achieving stable and repeatable deposition conditions in large-scale material extrusion additive manufacturing [3,6].

Extrusion pulsation can arise from several interacting process parameters, including screw rotation, material feeding, polymer rheology, temperature, and the pressure distribution within the extrusion system. In screw-based extrusion, the periodic movement of the screw geometry can generate pressure and flow pulsations at the screw-rotation frequency, which can subsequently affect the deposited strand geometry [5]. In addition to these screw-synchronous variations, longer-period fluctuations may arise from changes in material feeding, melt temperature, or other time-dependent process effects. The magnitude and characteristic behavior of these fluctuations can therefore depend on the extruder configuration, processing conditions, and polymer material [4,5,7,8].

Previous studies have investigated the monitoring and control of extrusion dynamics using process variables such as material flow, melt pressure, temperature, and extrusion speed. Pressure-based and feedback-controlled approaches have demonstrated the potential to compensate deviations from the desired extrusion state, while model-based and process-specific compensation strategies have also been investigated [4,6,9,10]. However, the extrusion dynamics depend on the material, extruder, nozzle geometry, and process conditions, which can limit the transferability of machine-specific control strategies. A directly measured process variable such as melt pressure therefore provides a potential basis for runtime compensation of extrusion variations. Recent studies have investigated pressure-based and feedback-controlled extrusion, including model-based and advanced feedback approaches for screw extrusion additive manufacturing [6,9,10].

In this work, melt pressure near the nozzle is investigated as a feedback variable for regulating material extrusion in a polymer-fed single-screw extruder. A synchronized measurement system combining nozzle pressure, screw position, conveyor position, and laser-based strand cross-section measurement is used to experimentally investigate the relationship between melt pressure and deposited strand geometry. Based on this relationship, proportional (P) and proportional–integral (PI) pressure controllers are implemented to adjust the physical extruder speed during continuous extrusion. A virtual E-axis and physical EE-axis architecture is used to separate the geometric extrusion demand defined by the G-code from the runtime extrusion correction. This allows process-state-dependent corrections to be applied without modifying the original geometric tool path. The objective of the study is to quantify the reduction in pressure-correlated extrusion pulsation and the resulting stabilization of the deposited strand cross-section.

2. Methods

2.1. Experimental Design and Measurement System

The experimental setup was designed to investigate extrusion pulsation by synchronously measuring the deposited strand geometry, melt pressure, screw position, and extruder operating data. In particular, the setup enables the relationship between internal melt pressure and the resulting deposited strand geometry to be evaluated during continuous extrusion.

The deposited strand was characterized using a conveyor-belt-based measurement system, as shown in Figure 1. The measurement concept is based on the authors' previously disclosed extrusion and measurement architecture [11], in which the extruded material is deposited continuously onto a servo-driven conveyor belt and the resulting strand geometry is measured along the deposition path. In the present study, this setup is used to investigate the relationship between melt pressure and the deposited strand cross-section during continuous extrusion. Direct material-flow measurements by collecting and weighing the extruded polymer were performed as independent reference measurements for validation of the laser-based flow estimation. Five independent measurements were conducted. The resulting material-flow rates showed agreement (>95%) with the flow rates determined from the laser-based measurements.

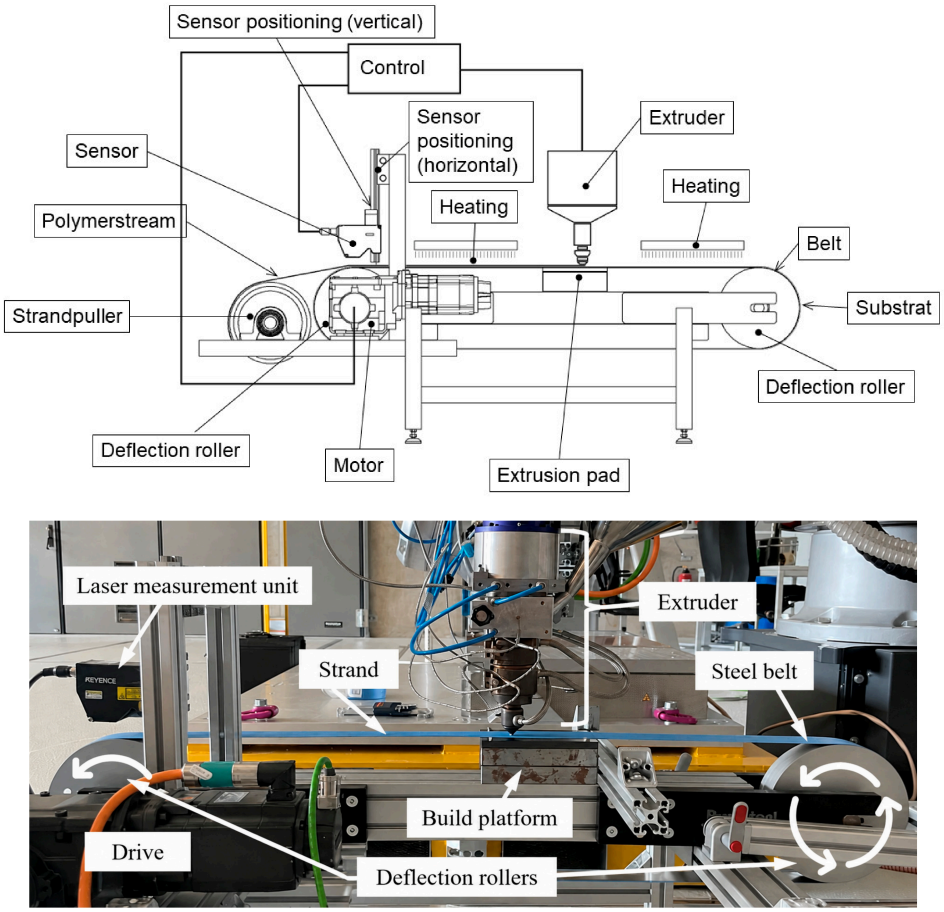

Figure 1. Experimental setup of belt measuring system.

The conveyor belt is driven by a servo motor, and its position is recorded synchronously with the NC (Numerical Control) data of the robotic system and the extruder. The conveyor belt is equipped with heating elements; however, the heating function was not used during the experiments presented in this study. A laser-line scanner is used to measure the cross-sectional geometry of the deposited strand. The laser measurements are acquired by an external Keyence (Osaka, Japan) measurement system. An electrical trigger generated by the NC controller provides the temporal synchronization between the laser measurements, the robotic control data, and the extruder data. The fixed distance between the nozzle position and the position of the measuring position was determined and taken into account during data analysis. Since the conveyor belt and the extruder are driven synchronously within the same NC system, the corresponding temporal offset between extrusion and laser measurement can be determined from the known distance and the conveyor-belt velocity

and applied to the measurement data. The measurement and deposition architecture follows the setup described in the authors' previous patent disclosure [11].

All measurement signals are sampled at a fixed interval of 8 ms, corresponding to a sampling frequency of 125 Hz. For the investigated screw speeds of 3–12 rpm, the corresponding screw-rotation frequencies are 0.05–0.2 Hz. The encoder is located at the motor, but the ratio of the gearbox is respected in the control system. The sampling frequency therefore provides approximately 625–2500 measurement samples per screw revolution and is sufficient to resolve the screw-synchronous fluctuations investigated in this study. At the conveyor-belt speed used in the experiments, the temporal sampling corresponds to a spatial sampling interval of approximately 0.26 mm along the deposited strand. The laser-line scanner provides a resolution of 0.1 mm in the x- and y-direction and 0.01 mm in the z-direction. Before the experiments, the scanner was calibrated using a flat reference surface.

The extruder motor is equipped with an encoder, allowing the absolute screw angle to be recorded and correlated with the measured melt pressure, deposited strand cross-section, and other control-system data. The drive data also provide information about the load acting on the screw. By synchronizing the screw position with the other measurement signals, pulsations associated with screw rotation can be distinguished from longer-period variations in the extrusion process.

The laser scanner was geometrically aligned and calibrated before the experiments to ensure reliable measurement of the deposited strand geometry. The scanner settings were defined during the machine calibration and kept constant throughout the experiments. Material-dependent optical and reflective properties can affect laser-based measurements; however, only PLA was investigated in the present study. A constant material feed to the extruder was maintained during the experiments to minimize feeding-related variations.

2.2. Single-Screw Extruder and Process Conditions

Large-scale material extrusion systems can employ different extrusion concepts, including single- and twin-screw extruders and melt-pump-based systems. Screw extruders may contain several functional zones, typically comprising a feed zone, a plasticization or compression zone, and a discharge or metering zone. Alternative plasticization concepts, such as auger-based systems with plate plasticization, are also used [3,5,12,13].

The experiments presented in this study were performed using a polymer-fed single-screw extruder. The extruder consists of a heated cylindrical barrel containing a single screw and a heated nozzle positioned at the outlet of the extrusion channel [5,13,14]. The extruder used in this study has two independently controlled heating zones. The screw conveys the solid polymer granules from the feed section through the plasticization region towards the discharge section before the melt enters the nozzle. The melt pressure reaches its highest level in the region near the nozzle entry point. After exiting the nozzle, the viscoelastic properties of the polymer can result in strand expansion [15,16].

An encoder integrated into the extruder drive provides the absolute angular position of the screw. The encoder signal is recorded synchronously with the melt pressure and deposited strand cross-section to investigate the relationship between screw rotation and extrusion pulsation. The drive system also provides information about the torque acting on the screw, which is recorded as an additional process variable.

The polymer material enters the extruder as solid granules. During conveying and plasticization, heat transfer and shear generated by the rotating screw cause the material to melt. The resulting extrusion behavior is influenced by the thermal and mechanical conditions within the extruder, including temperature, shear, and material residence time [8,17]. The viscosity of the polymer melt depends on process conditions including temperature

and shear rate [8]. The melt is subsequently conveyed through the channel at the screw tip and into the nozzle [15].

Thermoplastic melts exhibit both viscous and elastic behavior. When the melt passes through regions of decreasing cross-sectional area, elastic effects can become relevant [15,16]. During residence within the narrow nozzle channel, part of the deformation can relax. After exiting the nozzle, the remaining elastic contribution can cause expansion of the deposited strand. The magnitude of this effect depends, among other factors, on the residence time and flow conditions within the nozzle.

The main process variable used for feedback control in this study is the melt pressure. A Kistler 4004A105 MicroMelt sensor (Winterthur, Switzerland) with a measurement range of 0–500 bar is integrated directly into the nozzle near the extrusion channel (see Figure 2) and measures the local melt pressure at this position. The sensor position and integration into the flow channel were selected to minimize disturbances to the polymer flow. The pressure signal is recorded synchronously with the other process measurements and is used for both the pressure-strand cross-section correlation analysis and the closed-loop control experiments.

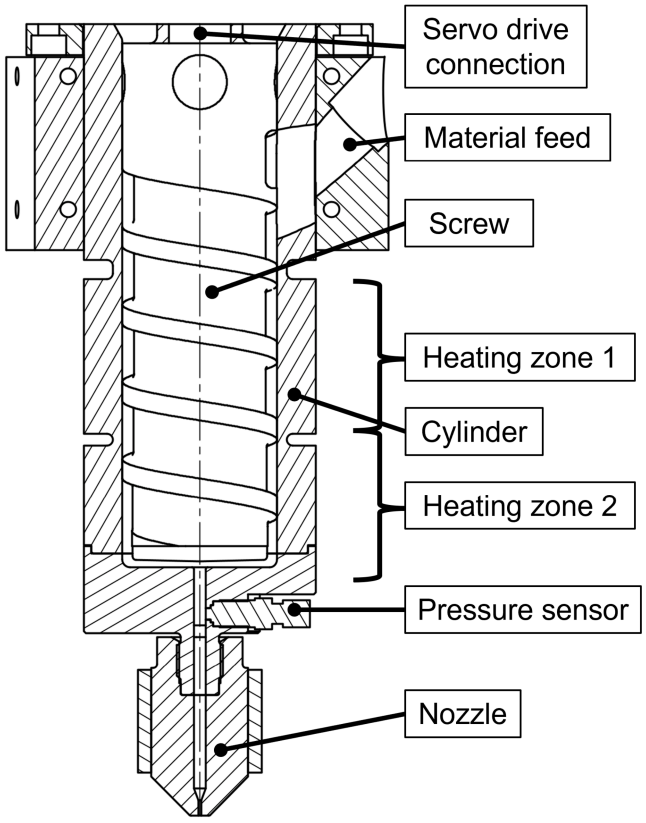

Figure 2. Single-screw extruder used for the experiments in the scope of this paper.

The experiments were conducted using a miniaturized extruder specialized for additive manufacturing, developed by Kunststoff-Zentrum Leipzig (KUZ). The extruder is operated using Siemens (Munich, Germany) SINAMICS drive technology. The single extrusion screw is controlled as one NC axis, providing the rotational position and drive data required for synchronization with the measurement system and for recording the extruder operating state.

2.3. G-Code Extrusion Setpoint and Control Architecture

This section discusses how the setpoint should be interpreted in a manner that respects the existing standard, aligns with accepted quality standards, and supports the objectives of this project.

According to the standard, the address letter E is designated for a second feed axis, representing a simultaneous but independent motion. However, the standard also allows for this address letter, if not used as specified, to be considered unassigned and available for custom applications. If no independent feed motion is specified, it is implicitly understood that the extruder movement is dependent on the geometry axes.

The G-code defines the target geometry and, consequently, the required material deposition along the programmed tool path. In conventional filament-based FDM/FFF processes, material extrusion is commonly represented by an interpolated E-axis [18,19]. In contrast, screw extruders often use a direct speed command for the extruder motor. Assuming the filament used has a defined diameter (e.g., 1.75 mm or 2.85 mm, as is typical for standard filament sizes), the setpoint for the filament path can be interpreted as a volumetric setpoint. The geometric axes (X, Y, Z) provide indirect information on layer height, path length, and extrusion width. Together, these parameters fully define the required setpoints and, for this reason, should also be used for screw extruders, even though these systems do not have a well-defined material cross-section. The setpoints at the start and end of extrusion are determined by the G-code setpoints and the specified dynamic limits of the involved mechanics (velocity, acceleration, jerk). All measurement values presented in this paper represent a segment with constant setpoints. Acceleration and deceleration processes were not considered in this work.

An additional and significant argument for defining the volumetric flow as a positional setpoint in G-code is the interpolative relationship between all positional axis setpoints. This means that the dynamic constraints (limits on speed, acceleration, and jerk) of all interpolated axes are jointly considered, ensuring that the system operates according to the capabilities of the slowest axis. A key advantage of this is that any reduction in path velocity—for example, when navigating corners of the geometry (Figure 3)—proportionally affects the extruder's speed setpoint. Similarly, this interpolation ensures that a sluggish extruder automatically results in an extended deceleration ramp for the geometry axes.

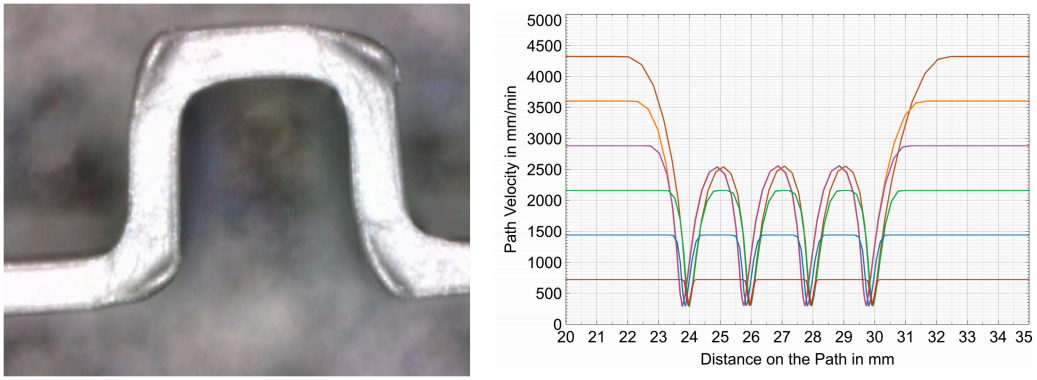

Figure 3. Illustration of the relationship between path velocity and extruder speed setpoint during cornering.

Figure 3 illustrates this kinematic relationship; it is not part of the experimental measurements used to evaluate extrusion pulsation. The E/EE-axis separation described here represents the implemented control architecture for separating the geometric extrusion demand from the runtime correction. Its behavior during acceleration, deceleration, and cornering was not experimentally evaluated in the present study.

With the procedure for generating setpoints, including all relevant dynamic boundary conditions, now established, the subsequent focus is on the relationship between the setpoint and the actual value. Since the interdependence of the involved axes is already embedded within the setpoint structure, it is sufficient to address the relationship between setpoint and actual value on a per-axis basis.

For screw extrusion, the relationship between extruder rotational speed and material flow depends on the operating conditions [8,10]. Consequently, corrections between the geometric setpoint and the motor setpoint are indispensable. In practice, parts of the additive manufacturing community implement such corrections directly within the CAM (Computer Aided Manufacturing) system or slicer. However, this approach inherently results in machine-specific G-code and cannot directly compensate for external process influences. The runtime pressure-feedback approach used in this study can potentially compensate for process disturbances that affect the measured melt pressure.

To overcome this limitation, this work adopts a different strategy. The G-code is designed to represent the unaltered target geometry, while all necessary corrections to achieve this desired geometry are applied at runtime within the control system itself. However, this leads to new challenges. Any correction applied to the extrusion directly alters the system's dynamic behavior. If the interpolation process generates extruder-axis setpoints already at the limit of the system's capabilities, and subsequent corrections require further increases, this inevitably results in overloading the axis.

To resolve this issue, this research introduces a conceptual separation between two extruder axes. The first axis, denoted as E, is utilized solely within the interpolator to coordinate with the other motion axes, while the second axis, denoted as EE, represents the physical extruder. The interpolator axis E is treated as a purely virtual axis. The dynamic behavior of the physical axis EE results from the intrinsic properties of the extruder, whereas the dynamics of the virtual axis E are defined by those of EE in combination with the correction values (Figure 4).

$$u_{EE} = u_E + \Delta u_{control} \quad (1)$$

Here, u_E denotes the extrusion command generated by the virtual E-axis, $\Delta u_{control}$ the correction generated by the process-control system, and u_{EE} the resulting command applied to the physical extruder axis [13]. This concept allows for arbitrary correction values to be incorporated, effectively decoupling the relationship between setpoint and actual value for material extrusion, without violating the system's dynamic constraints.

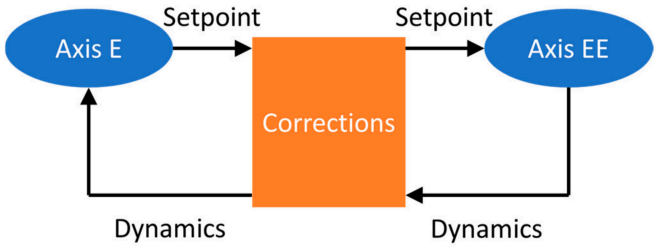

Figure 4. Control concept.

3. Results and Discussion

Correlation Analysis: To assess the short- and long-term extrusion characteristics and to gather data for a systematic control approach, ten-minute intervals are recorded with constant screw and belt speed per trial. Axial extruder speed is varied to cover a wide range of stable operating conditions. Transient behavior after start-up or parameter changes is closely monitored and excluded from the test intervals to avoid any distortion of the measured data.

The recorded data for all steady-state tests shows superposed pulsations of different frequencies which appear to be related to the prevailing screw speed. Figure 5 shows data in reference to the screw position with recorded cross-sectional area as well as pressure and drive load of the extruder. Similar curve appearance in relation to the screw angle can be observed in all the tests performed, indicating a direct connection of the phenomena to the screw position. An experiment with the material feed running empty rules out the material feed as a major contributor to the pulsations observed in this paper. The Pearson correlation coefficient between melt pressure and strand cross-sectional area is shown in Figure 6. The Pearson correlation was calculated using the steady-state measurement intervals. The temporal offset between the nozzle and the laser measurement position was compensated during data analysis based on the known distance between the two positions and the conveyor-belt velocity. Since the conveyor belt and extruder were synchronized within the same NC system, the corresponding time shift could be determined and applied to the measurement data.

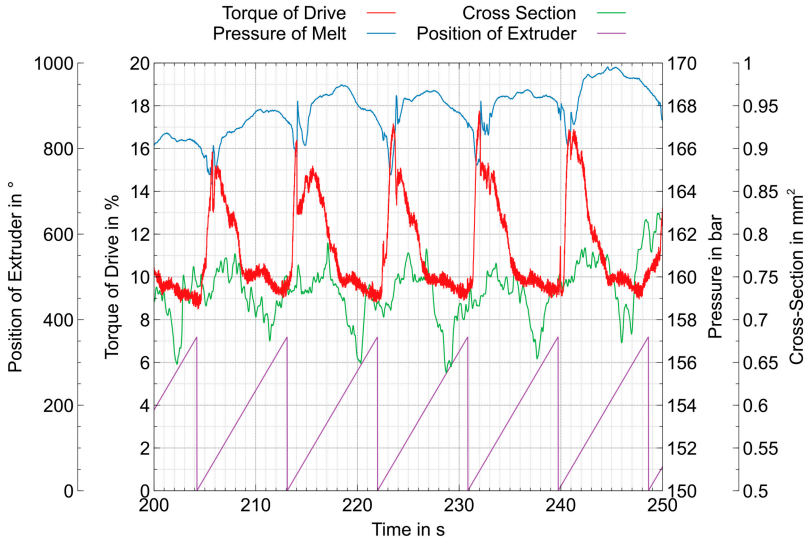

Figure 5. Measured screw position, cross-sectional area, melt pressure and drive torque.

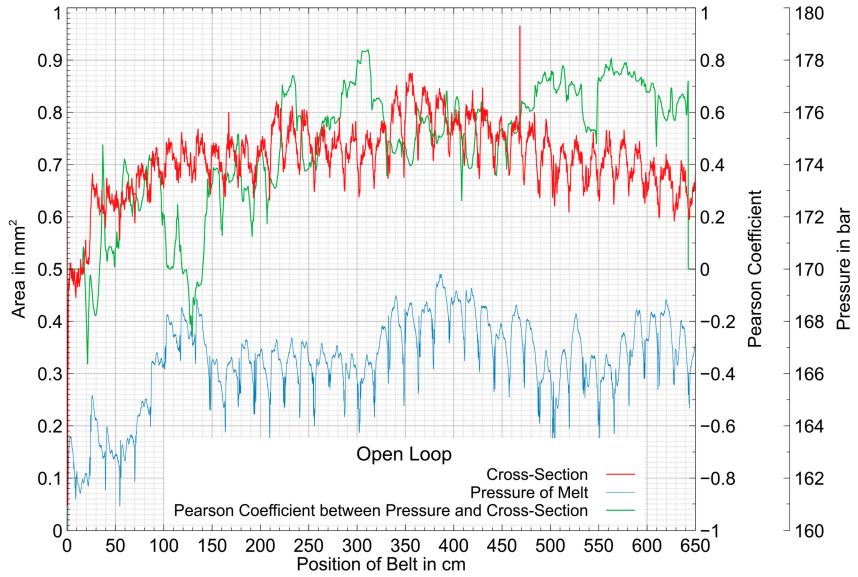

Figure 6. Pearson correlation between melt pressure and deposited strand cross-sectional area.

The theoretical foundation of this work is based on the Hagen–Poiseuille law, which describes the influencing factors of material flow through a circular cylindrical nozzle. The Hagen–Poiseuille relationship is formally valid for Newtonian fluids, whereas polymer melts exhibit non-Newtonian and viscoelastic behavior. Therefore, Equation (2) is not used as a predictive model of the extrusion process. Instead, it provides a simplified physical basis for considering melt pressure as a flow-related process variable. Within the scope of this paper, it is assumed that the governing factors for non-Newtonian fluids [12] include, at a minimum, those described by the Hagen–Poiseuille law [20].

$$\dot{\mathbf{V}} = \frac{\Delta \mathbf{p} \boldsymbol{\pi} \mathbf{d}^4}{(128 \boldsymbol{\eta} \mathbf{l})} \quad (2)$$

The nozzle outlet diameter (d) is difficult to vary and the dynamic viscosity ($\boldsymbol{\eta}$) is dependent on factors such as temperature and shear rate. Pressure drop along the nozzle axis appears to be a suitable control parameter to compensate for material-flow fluctuations.

In the following, the relationship between the pressure profile at a fixed position near the extruder nozzle outlet and the material flow is determined empirically. For this purpose, with a constant screw speed per trial and after allowing sufficient settling time, both material flow and pressure were measured over several screw rotations.

The experiments are conducted using spherical PLA granules, showing reliable and consistent feeding behavior in previous projects. The nozzle-to-conveyor-belt distance was set to $\mathbf{t} = \mathbf{1.0}$ mm.

The observation of longer-period pressure and mass-flow variations is nevertheless consistent with previously reported pulsation phenomena in single-screw extrusion [5,6]. The analysis of the geometric data from the line laser measurements reveals a strong correlation between the width, height, and cross-sectional area of the measured polymer strands. The cross-sectional area proves to be the most robust parameter in the presence of measurement errors. Consequently, the subsequent analysis focuses on the cross-sectional area to simplify data interpretation. Material flow was not measured by a conventional in-line flow sensor. Instead, a laser scanner measured the geometry of the deposited strand, from which the strand cross-sectional area was determined as a flow-related process indicator.

The correlation of measured pressure and cross section data in the time domain signal can be quantified with a Pearson after the swing-in phase. The used window for the gliding Pearson correlation is set to one screw rotation. Correlation coefficient up to $r_{p,p-A} > 0.8$ confirms the visually apparent correlation. In addition to the periodicity synchronized with the screw rotation, longer periodic fluctuations are also observed; however, these are not investigated further in the scope of this work.

The results of the preliminary experiments are consistent with the general observations reported in the literature on single-screw extrusion, such as those by Chung [13] and Hopmann [14], confirming the occurrence of pulsations in both mass flow and pressure. Moreover, the systematic variation in process parameters, such as screw speed, conveyor-belt speed, and material feed rate, provide insights regarding the influence of individual process variables. This improved understanding of both the extruder and the measurement system's capabilities directly supports the design and refinement of subsequent experiments.

Control setup: Both the observed correlation between pressure and material flow and the implications of the Hagen–Poiseuille law suggest that maintaining a constant pressure at a fixed position within the nozzle should result in a steady material flow. A constant outlet pressure in the nozzle should result in a steady material flow. The measurements indicated that the correlation between pressure and material flow was stronger than the periodicity linked to the screw-rotation position. Therefore, as an initial approach, the decision is made to refrain from implementing a feedforward control strategy based on the extruder position for pressure control aimed at reducing material-flow pulsations. In the

present study, nozzle melt pressure is used as the feedback variable. The pressure-based control architecture was previously disclosed by the authors [21].

For the pressure-controlled experiments, a predefined pressure setpoint was specified for each extrusion condition. The extruder screw speed was adjusted by the controller according to the deviation between the measured nozzle melt pressure and the corresponding pressure setpoint. The measured pressure was compared with this setpoint, and the resulting control error was used to adjust the extruder screw speed, as illustrated in Figure 7.

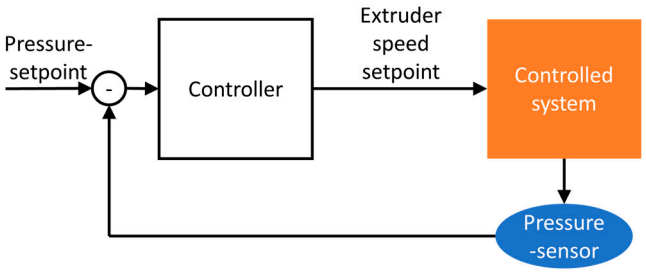

Figure 7. Control setup for robotic printing system.

The control loop uses the measured nozzle melt pressure as its sole feedback signal. The laser scanner measurement of the deposited strand geometry is not used for feedback control. Instead, the measured strand cross-sectional area is used to determine the deposited strand cross-sectional area and to evaluate the resulting extrusion stability. The screw encoder signal is used to relate the measured process signals to the screw position and to identify screw-synchronous pulsation, while the motor torque is recorded for process monitoring. Neither the laser-based cross-sectional area, the screw angle, nor the motor torque is used to calculate the correction of the extruder screw speed.

The control error is determined from the difference between the defined pressure setpoint and the measured nozzle melt pressure. The P/PI controller uses this pressure error to calculate a correction to the extruder screw-speed command. The strand cross-sectional area is therefore used exclusively as an evaluation variable and does not enter the control loop directly.

For the quantitative evaluation of extrusion pulsation, the variation in the deposited strand cross-sectional area is evaluated from the laser measurements. This quantity is used to assess the effectiveness of the pressure-control strategy but is not used by the P/PI controller itself. The controller therefore regulates the nozzle melt pressure, while the resulting variation in strand cross-sectional area is used to evaluate the effect of the control strategy on material deposition.

A proportional (P) controller was first implemented because of its straightforward implementation and fast response. The proportional gain was experimentally varied within the final operating range to assess the stability of the control response. Higher gain values resulted in oscillatory or unstable behavior; therefore, the gain was reduced until stable operation was achieved. A proportional gain of $K_P = 0.1$ rpm/bar was selected for all experiments presented in this study. The controller was subsequently extended to proportional–integral (PI) control to reduce the steady-state pressure deviation. The integral gain was varied experimentally around the final operating range. The integral contribution was increased until oscillatory behavior occurred and subsequently reduced to the highest value that resulted in stable operation. The integral gain used for the experiments was $K_I = 0.0012$ rpm/bar. This empirical tuning procedure was selected because no prior identified dynamic model of the investigated extruder was available.

As a result, improved pressure stability is achieved, while the characteristic steady-state error typical for proportional controllers remains (Figures 8 and 9).

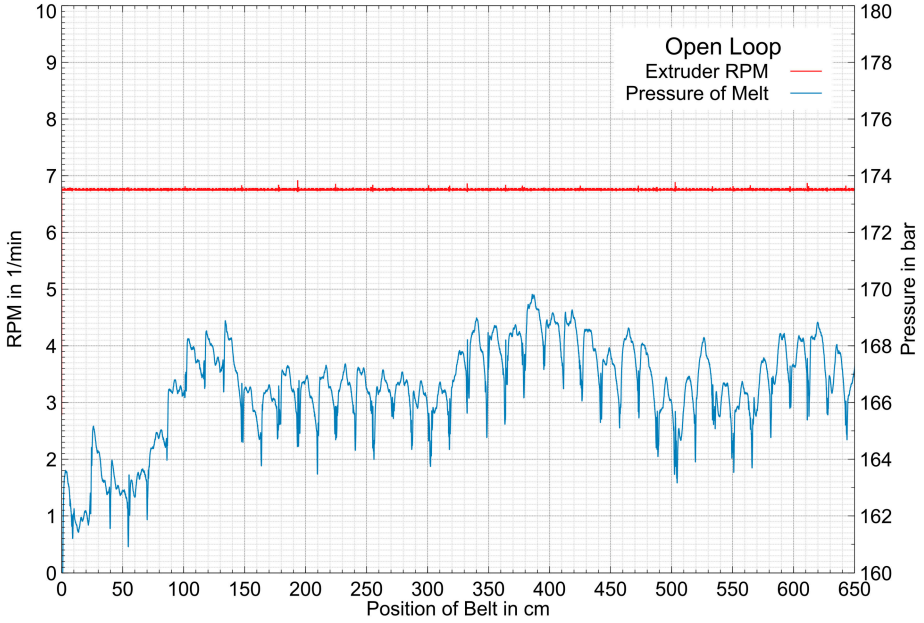

Figure 8. Pressure and extruder speed without control mechanism.

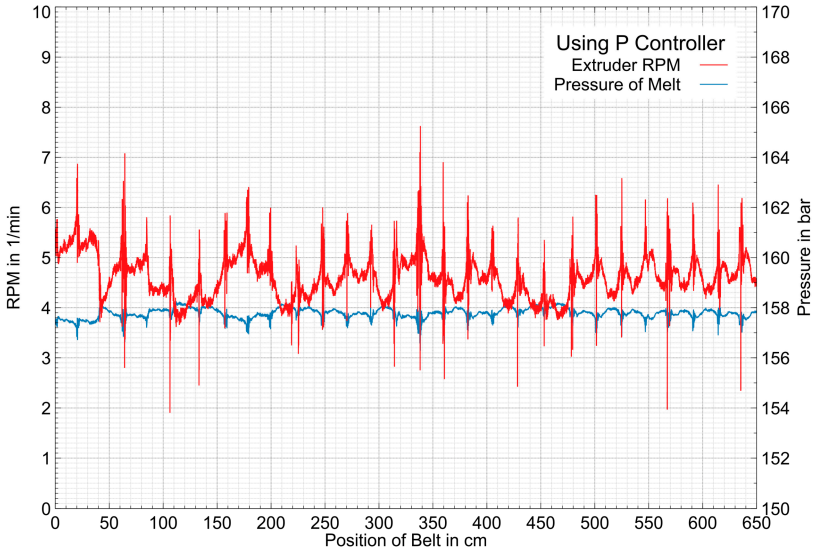

Figure 9. Pressure and extruder speed with P-control.

An effective control of the extruder screw speed is observed, maintaining the setpoint pressure effectively. Nevertheless, both short-cycle fluctuations (synchronized with the screw rotation) and long-cycle fluctuations remain. The pressure fluctuations are reduced by approximately 80% in the long term. To further minimize the remaining deviations in the pressure profile, the controller is extended to a PI-controller. These values were determined empirically for the investigated extruder, material, nozzle, and sensor configuration and should therefore not be considered directly transferable to other system configurations. As a result, pressure stability is quantified (Figure 10).

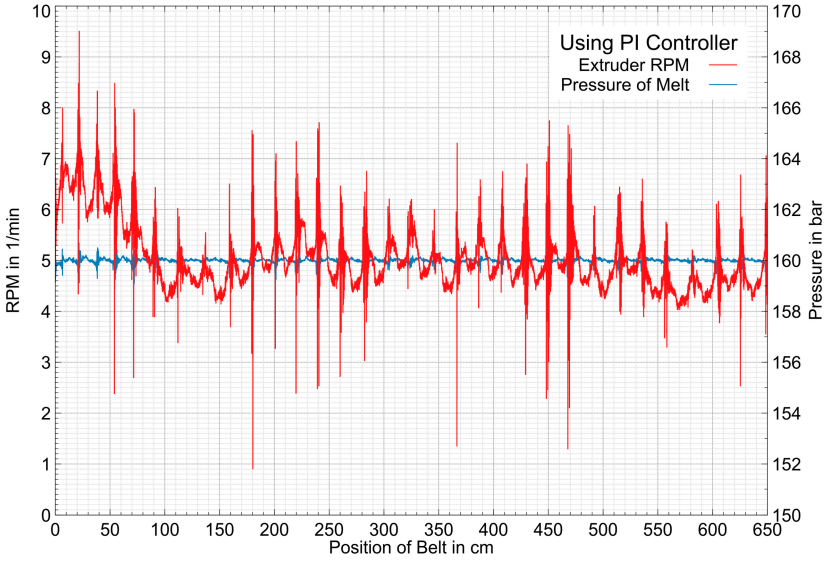

Figure 10. Pressure and extruder speed with PI-control.

The correlation with pressure was greater in the preliminary trials than with screw position, so pressure control appeared more promising than sensorless feedforward control based on screw position.

No digital filtering was applied to the pressure signal during controller operation. The raw pressure signal was therefore used directly by the controller at the applied sampling frequency of 125 Hz. Preliminary measurements were considered sufficiently stable without additional filtering, and no filter was introduced into the control loop. The short-term variations in the commanded extruder speed result from the direct response of the controller to the instantaneous pressure error. Since the raw pressure signal is used without digital filtering, short-term pressure variations are directly reflected in the extruder speed command. No additional filtering or rate limitation of the extruder speed command was applied in the present study in order to preserve the direct response of the pressure-feedback loop. The potential influence of filtering or rate limiting on the control performance was not systematically investigated. The peaks in Figures 9 and 10 correlate with the full rotations of the screw.

The implementation of the PI-controller does not lead to a further reduction in the pressure fluctuation amplitude. However, the actual pressure now corresponds to the setpoint in terms of its arithmetic mean.

Validation test: Different target strand widths are generated by varying extruder screw speed. This effectively increases the ratio of belt feed per extruder rotation (slow 45/250 [°distance/°screw rotation], medium 45/350, high 45/450). The actual belt speed can be calculated with this ratio and the extruder rpm displayed, e.g., in Figures 9 and 10. For the pressure-controlled experiments, pressure setpoints of 160, 165, and 170 bars were used for the low-, medium-, and high-speed conditions, respectively. The pressure setpoints were determined in preliminary trials. The conveyor-belt speed was adjusted proportionally to the extrusion speed for the investigated conditions, maintaining the same relative velocity between the deposited material and the conveyor belt. This ensured that the deposited strand was neither stretched nor compressed during deposition. In all diagrams, the measured pressure, cross-sectional area of the material strand and extruder screw speed are plotted with respect to the belt position. Variations in the strand cross-section manifest themselves in the component as varying wall thicknesses and, consequently, geometric deviations, as well as optically uneven surfaces. Measuring the cross-section is therefore a good method for assessing the effects of material flow on component quality. Due to the

small magnitude and dynamic nature of the extrusion pulsation, the resulting variations in strand geometry are difficult to assess reliably by visual inspection. The screw-induced pulsation corresponds to approximately 12% variation over a strand length of about 15 cm based on the measurements presented in this study, which is difficult to detect reliably by eye or in a photograph. Therefore, the effect of pressure control is quantitatively evaluated using the laser-based measurements of the deposited strand cross-sectional area.

With low extruder speed a strand width of approximately 2 mm is observed. The pulsation, which is synchronized with the screw rotation, is visibly reflected in both the pressure and the material cross-sectional area (Figure 11A).

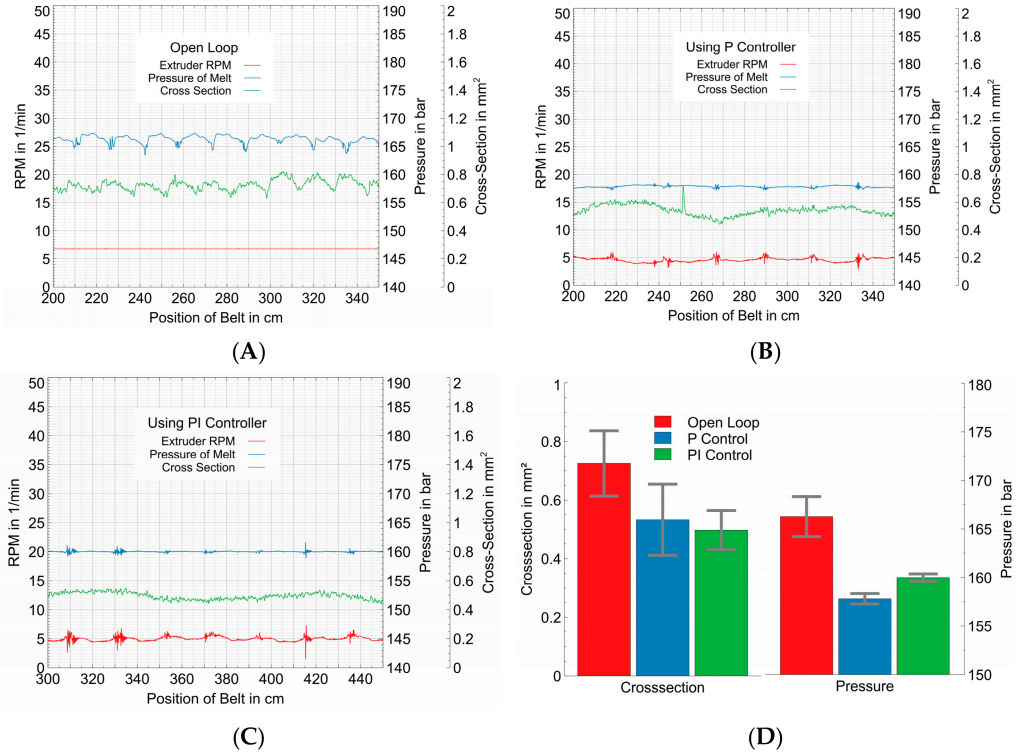

Figure 11. Extruder speed, pressure and cross-sectional area for slow printing speeds. (**A**) Without control; (**B**) with P-control; (**C**) with PI-control; and (**D**) statistic.

The proportional control modulates the extruder screw speed, resulting in significantly more stable pressure and material cross-section. The graph consists of pulsation synchronized with the screw rotation, resulting from the extruder turns, and additional pulsation asynchronous with the screw rotation, as well as pulsations that are asynchronous with screw rotation. However, asynchronous pulsations remain (Figure 11B). The small pressure peaks are not visible in cross section data. At belt position 250, a sudden drop in the material cross-section is observed, which can be attributed to a measurement error caused by contamination of the belt.

As expected from the PI-controller, the pressure remains constant in the arithmetic mean throughout the entire process, effectively linearizing the material flow (Figure 11C).

For each extrusion-speed condition, one measurement campaign was conducted over the specified measurement period. The statistical values shown in Figures 11D–13D were calculated from the data recorded during the respective campaign, comprising multiple screw revolutions. The error bars represent the standard deviation of the recorded values over the evaluated measurement interval. The mean values for the controlled experiments are lower than those for the uncontrolled reference condition. This difference is consistent with the lower pressure levels used in the pressure-controlled experiments. Therefore, the

controlled and uncontrolled conditions do not represent strictly identical mean-pressure or material-throughput conditions. The resulting differences in the mean strand cross-sectional area should therefore be distinguished from the reduction in extrusion pulsation. Although the standard deviation of the controlled pressures is significantly lower, the standard deviation of the strand cross-sectional areas is reduced only to a limited extent. In conjunction with the curves, this suggests that the control system completely suppresses the pulsation occurring synchronously with the screw, whereas the pulsation occurring asynchronously with the screw remains.

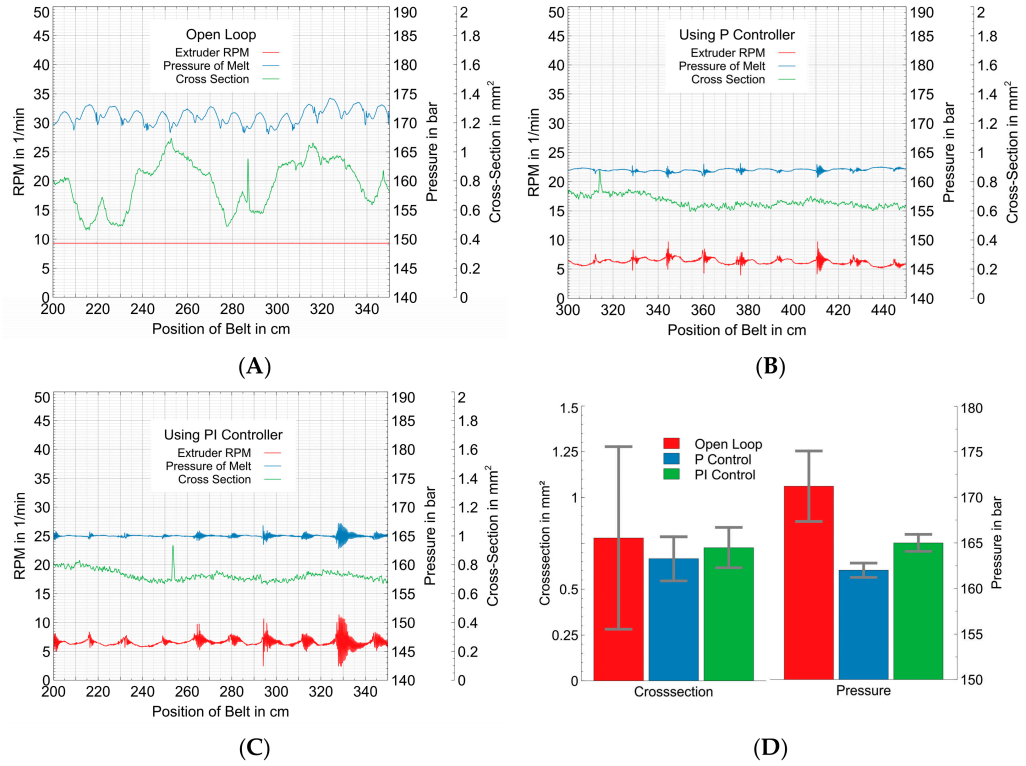

Figure 12. Extruder speed, pressure and cross-sectional area for medium printing speeds. (**A**) Without control; (**B**) with P-control; (**C**) with PI-control; and (**D**) statistic.

At medium extruder speed a width of approximately 2.4 mm was produced. In addition to the extruder-synchronized pulsation, an increase in asynchronous oscillation is observed (Figure 12A).

With the P-controller, these pulsations asynchronous with the screw-rotation oscillations are also greatly reduced compared to the results without control (Figure 12B). A downward trend in the material cross-section is noticeable, which does not correlate with the pressure. One possible explanation for the observed downward trend is a change in melt viscosity during the experiment, for example due to thermal drift or material-related effects such as moisture. At a given pressure level, changes in melt viscosity can affect the resulting material throughput and therefore the deposited strand cross-sectional area. However, temperature, moisture content, and viscosity were not independently measured in the present experiments. Therefore, this explanation remains a possible interpretation and cannot be verified from the available data.

Similar to the measurements with the PI-controller, a downward trend in the material cross-section is noticeable at medium extruder speeds (Figure 12C).

At medium extruder speed, the lower mean strand cross-sectional area in the pressure-controlled experiments is consistent with the lower pressure setpoint used for this condition (Figure 12D). The pronounced oscillations asynchronous with screw rotation are reduced

by the control system to approximately one-third of their magnitude in the uncontrolled condition, both in melt pressure and strand cross-sectional area, as indicated by the corresponding standard deviations. A strand width of approximately 3 mm is observed for high extruder speeds. The pulsation asynchronous to the screw rotation no longer decays (Figure 13A).

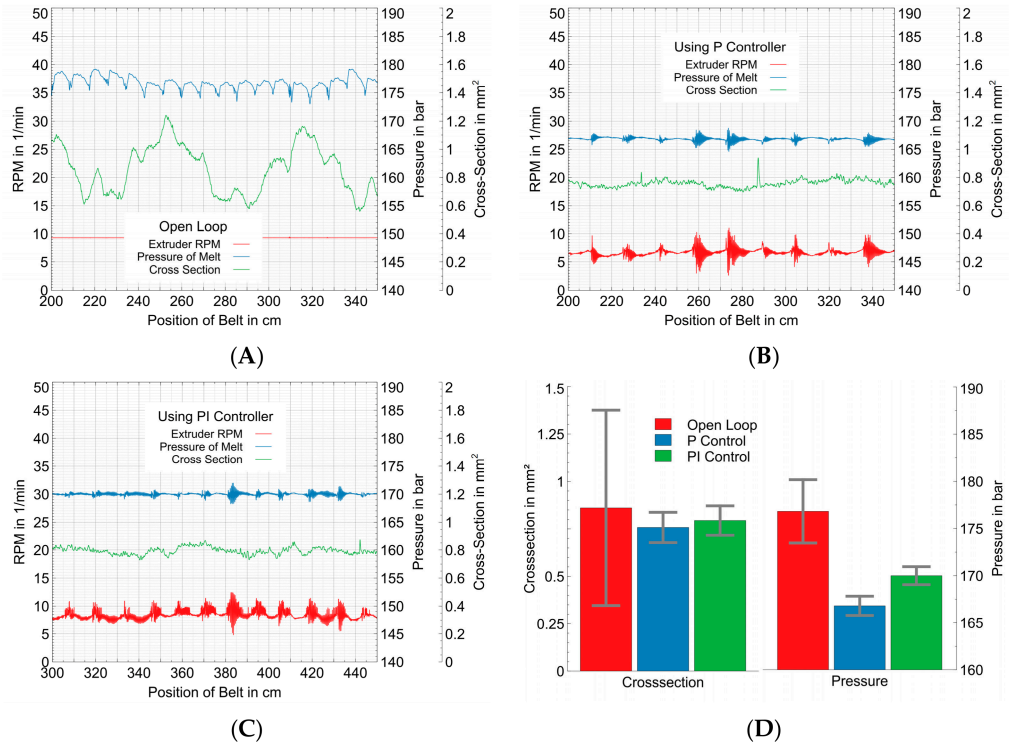

Figure 13. Extruder speed, pressure and cross-sectional area for high printing speeds. (**A**) Without control; (**B**) with P-control; (**C**) with PI-control; and (**D**) statistic.

The measurements confirm the results obtained with the P-controller at medium extruder speed (Figure 13B).

The modulation of the extruder screw speed appears highly dynamic (Figure 13C). The results are consistent with the findings of previous measurements.

At high extruder speed, the lower mean strand cross-sectional area in the pressure-controlled experiment is likewise consistent with the lower pressure level defined for this condition (Figure 13D). The more pronounced oscillations of the strand cross-section, which are not synchronized with the movement of the extruder or with the pressure fluctuations, contrast with the proportionally greater suppression of oscillations in the strand cross-section observed in the experiments with the pressure controller.

4. Conclusions

This study investigated pressure-based feedback control as a method for reducing extrusion pulsation in a polymer-fed single-screw extruder for direct-extrusion additive manufacturing. An experimental setup combining synchronized nozzle-pressure measurement, screw-position measurement, conveyor-belt tracking, and laser-based strand cross-section measurement was used to characterize the relationship between melt pressure and deposited strand geometry.

The measurements revealed a strong correlation between nozzle melt pressure and deposited strand cross-sectional area, with a Pearson correlation coefficient up to $r > 0.8$. The results further showed that a significant component of the observed strand-geometry

modulation is synchronized with screw rotation. This screw-synchronous component was strongly suppressed when pressure-based feedback control was applied.

The runtime pressure-control architecture was evaluated using proportional (P) and proportional–integral (PI) control. At the investigated medium extrusion speed, P-control reduced the remaining deposited strand cross-sectional modulation to approximately 33% of the corresponding uncontrolled reference condition. PI-control did not provide a further substantial reduction in the remaining strand cross-sectional modulation compared with P-control, but improved the mean-pressure tracking and thereby reduced the steady-state pressure deviation.

The experiments at different extrusion conditions showed that pressure feedback can reduce pressure-correlated variations in the deposited strand cross-section over the investigated range of PLA operating conditions. At the same time, additional variations in strand geometry remained even when the measured pressure was relatively stable. In particular, the downward trend observed in the strand cross-sectional area at some operating conditions could not be explained by the measured pressure. Its underlying cause cannot be determined from the present experiments and may be related to additional thermal, feeding, moisture-related, or rheological effects. Temperature, moisture content, and melt viscosity were not independently measured and therefore cannot be identified as the cause from the available data.

The present study was limited to PLA, a fixed nozzle-to-conveyor-belt distance, and the investigated range of extrusion conditions. The transferability of the proposed approach to other thermoplastics, different nozzle geometries, deposition conditions, and filled or fiber-reinforced materials therefore requires further investigation. Similarly, the present experiments focused on quasi-steady extrusion intervals; start-up, shutdown, and long-duration multi-hour printing were not quantitatively evaluated.

The separation between the virtual extrusion demand and the physical extruder command enables pressure-based runtime corrections to be applied during deposition while maintaining the geometric extrusion demand defined by the G-code. However, the behavior of this architecture during acceleration, deceleration, and cornering was not experimentally evaluated in the present study. The control approach is model-independent and does not require a predictive dynamic model of the extruder. The results therefore demonstrate the feasibility of using nozzle melt pressure as a feedback variable for reducing pressure-correlated extrusion pulsation in screw-based additive manufacturing.

Future work should investigate the remaining sources of strand-geometry variation, systematic controller tuning, longer-duration operation, different polymer materials and nozzle configurations, and direct validation of the resulting improvements in final-part dimensional accuracy, surface quality, and internal structure.

Author Contributions: Conceptualization, J.-U.R.S. and J.J.; methodology, J.-U.R.S., J.J. and S.B.; software, J.J., S.B. and R.K.; validation, J.-U.R.S., J.J., S.B. and R.K.; formal analysis, J.-U.R.S., J.J., S.B. and R.K.; investigation, J.-U.R.S., J.J., S.B. and R.K.; resources, H.P.M. and H.Z.; data curation, J.-U.R.S., J.J. and S.B.; writing—original draft preparation, J.-U.R.S., J.J. and S.B.; writing—review and editing, J.-U.R.S., J.J. and S.B.; visualization, J.J. and R.K.; supervision, J.-U.R.S. and M.T.; project administration, J.-U.R.S. and M.T.; funding acquisition, J.-U.R.S. and M.T. All authors have read and agreed to the published version of the manuscript.

Funding: This research received no external funding.

Data Availability Statement: The data presented in this study are available from the corresponding author upon reasonable request.

Acknowledgments: The authors gratefully acknowledge Siemens AG and the DLR Strategic Field AddCompS®—Additive Composite Structures for providing the technical infrastructure and support for this work.

Conflicts of Interest: The authors declare a potential competing interest related to patent applications [11,21], which concern methods relevant to the work presented in this manuscript and were filed through the German Aerospace Center (DLR). Siemens AG was involved in the experimental work through the contribution of one of the authors. Siemens AG provided no financial support or equipment for this study. The role of Siemens AG and the relationship of the authors to the patent applications are disclosed for transparency.

Abbreviations

The following abbreviations are used in this manuscript:

AM	Additive Manufacturing
CAM	Computer-Aided Manufacturing
DLR	German Aerospace Center
E	Virtual Extruder Axis
EE	Physical Extruder Axis
FDM	Fused Deposition Modeling
FFF	Fused Filament Fabrication
G-code	Numerical Control Programming Language
NC	Numerical Control
P	Proportional Controller
PI	Proportional–Integral Controller
PLA	Polylactic Acid
rpm	Revolutions per Minute

References

1. Bhatt, P.M.; Malhan, R.K.; Shembekar, A.V.; Yoon, Y.J.; Gupta, S.K. Expanding capabilities of additive manufacturing through use of robotics technologies: A survey. *Addit. Manuf.* **2020**, *31*, 100933. [CrossRef]
2. Toshev, R.; Bengs, D.; Helo, P.; Zamora, M. Advancing Free-Form Fabrication: Industrial Robots' Role in Additive Manufacturing of Thermoplastics. *Procedia Comput. Sci.* **2024**, *232*, 3131–3140. [CrossRef]
3. Altıparmak, S.C.; Yardley, V.A.; Shi, Z.; Lin, J. Extrusion-based additive manufacturing technologies: State of the art and future perspectives. *J. Manuf. Process.* **2022**, *83*, 607–636. [CrossRef]
4. Colon, A.R.; Kazmer, D.O.; Peterson, A.M. The dependency chain in material extrusion additive manufacturing: Shaft torque, infeed load, melt pressure, and melt temperature. *Addit. Manuf.* **2023**, *77*, 103780. [CrossRef]
5. Campbell, G.A.; Spalding, M.A. *Analyzing and Troubleshooting Single-Screw Extruders*, 2nd ed.; Carl Hanser Verlag: München, Germany, 2021.
6. Kunz, B.; Mößner, K.; Werner, R. Measurement, modeling, and control of extrusion dynamics in FFF 3D printing. *Prog. Addit. Manuf.* **2026**, *11*, 6541–6554. [CrossRef]
7. Janßen, M. Frei Rotierende Systeme in der Einschneckenextrusion. Doctorate Dissertation, Universität Duisburg-Essen, Duisburg, Germany, 2023.
8. Yu, L.-M.; Huang, H.-X. Temperature and shear dependence of rheological behavior for thermoplastic polyurethane nanocomposites with carbon nanofillers. *Polymer* **2022**, *247*, 124791. [CrossRef]
9. Zimenko, K.V.; Afanasev, M.Y.; Kolesnikov, M.V. Pressure control in material extrusion additive manufacturing. *Sci. Tech. J. Inf. Technol. Mech. Opt.* **2022**, *22*, 929–940. [CrossRef]
10. Ma, Y.; Li, X.; Ma, N.; Yao, Y.; Wang, S.; Hu, Z. Precise pressure control for screw extrusion 3D printing of PP-GF composites based on inverse model feedforward and variable structure feedback. *Materials* **2026**, *19*, 1453. [CrossRef] [PubMed]
11. Johannsen, E.; Titze, M.; Schmidt, J.-U. Mess-/Depositionseinrichtung für die Additive Fertigung. DE 10 2023 127 678 A1, 2023, 24 April 2025.
12. Bender, B.; Göhlich, D. (Eds.) *Dubbel—Taschenbuch für den Maschinenbau, Band 2: Anwendungen*, 26th ed.; Springer Vieweg: Berlin/Heidelberg, Germany, 2020; 717p.
13. Chung, C. *Extrusion of Polymers—Theory and Practice*, 3rd ed.; Carl Hanser Verlag: München, Germany; Wien, Austria, 2020.
14. Hopmann, C.; Michaeli, W. *Einführung in die Kunststoffverarbeitung*; Carl Hanser Verlag: München, Germany; Wien, Austria, 2017.

15. Serdeczny, M.P.; Comminal, R.; Pedersen, D.B.; Spangenberg, J. Experimental and analytical study of the polymer melt flow through the hot-end in material extrusion additive manufacturing. *Addit. Manuf.* **2020**, *32*, 100997. [CrossRef]
16. Zhang, H.; Ye, F.; Chen, F.; Yuan, W.; Yan, W. Numerical investigation on the viscoelastic polymer flow in material extrusion additive manufacturing. *Addit. Manuf.* **2024**, *81*, 103992. [CrossRef]
17. Radwan, M.; Schneider, S.; Müller, T.E.; Frerich, S. Understanding the dynamics of polymer extrusion: Simulation of thermoplastics processing with planetary roller extruders. *Heliyon* **2024**, *10*, e28729. [CrossRef] [PubMed]
18. Roschli, A.C.; Borish, M.C.; Feldhausen, T.A.; Barnes, A.K.; Wang, P.L.; Macdonald, E.W. The G-code file. In *Motion and Path Planning for Additive Manufacturing*; Roschli, A.C., Borish, M.C., Barnes, A.K., Wang, P., Macdonald, E., Eds.; Elsevier: Amsterdam, The Netherlands, 2024; pp. 225–239.
19. Jin, Y.-A.; He, Y.; Fu, J.-Z.; Gan, W.-F.; Lin, Z.-W. Optimization of tool-path generation for material extrusion-based additive manufacturing technology. *Addit. Manuf.* **2014**, *1–4*, 32–47. [CrossRef]
20. Eu, B.C. Generalization of the Hagen–Poiseuille velocity profile to non-Newtonian fluids and measurement of their viscosity. *Am. J. Phys.* **1990**, *58*, 83–84. [CrossRef]
21. Titze, M.; Johannsen, E.; Schmidt, J.-U. Druckbasierte Regelung Eines Extrusionsprozesses für die Additive Fertigung DE 10 2023 127 672 A1, 2023, 4 April 2025.

Disclaimer/Publisher's Note: The statements, opinions and data contained in all publications are solely those of the individual author(s) and contributor(s) and not of MDPI and/or the editor(s). MDPI and/or the editor(s) disclaim responsibility for any injury to people or property resulting from any ideas, methods, instructions or products referred to in the content.